Numerical Simulation for Flow Field Characteristics of Swirling Flow with and without Combustion

H. M. Gad*, A. M. Elzallat*, T. M. Farag*, I. A. Ibrahim*

*Mechanical Power Engineering Department, Faculty of Engineering, Port Said University, Port Said, Egypt

(hamada_zzdd@eng.psu.edu.eg, zallat2@yahoo.com, faragtm@yahoo.com, eng.hema@eng.psu.edu.eg)

Corresponding Author: Hamada Mohamed Gad, Mechanical Power Engineering Department, Faculty of Engineering, Port Said University, Port Said, Egypt, Phone: +201007254810, Fax: +20663400936, E-mail: hamada_zzdd@eng.psu.edu.eg

Received: 12.09.2021 Accepted:04.10.2021

Abstract- The present study presents a numerical investigation of the effects of swirl number on gaseous fuel combustion characteristics and the cold flow field. A numerical simulation of the diffusion natural gas flames is presented in a 3-D combustor tube model. Computational Fluid Dynamics (CFD) studies are carried out by ANSYS FLUENT package version 14.5. Seven swirl numbers; S = 0, 0.23, 0.5, 0.87, 1.5, 2 and 3 are used at excess air factors of 2.0 and 4.0 with constant inlet fuel mass flow rate at 0.4 g/s. The obtained numerical results are introduced to clarify the effects of the changing swirl number on the cold flow field and the combustion characteristics, such as the Reverse Flow Zone (RFZ), circulation vortex eye position, flow pathlines, recirculated air flow mass ratio, flame temperatures distributions, and combustion products concentrations. The obtained results show that when increasing the swirl number and the excess air factor, the size of the Central Reverse Flow Zone (CRFZ) and the central vortex increased, the flame length decreased, the recirculated flow mass ratio increased and the average percentage of CO and unburnt fuel (CH_4) concentration at the combustor tube end decreased.

Keywords Numerical simulation, natural gas combustion, diffusion flame, swirling flow, emissions.

Nomenclature and abbreviations

A/F	Air to fuel mass ratio
CRFZ	Central Reverse Flow Zones
$\dot{m}_a$	Combustion air mass flow rate, g/s
$\dot{m}_f$	Fuel inlet mass flow rate, g/s
$\dot{m}_i$	Total inlet mass flow rate, g/s
$\dot{m}_r$	Reversed mass flow rates, g/s
RFZ	Reverse Flow Zone
R_i	The hub (inner) radii of the swirler, mm
R_o	The outer radii of the swirler, mm
r/D	Dimensionless radial distance
S	Air swirl number
T_{inlet}	Inlet temperature, K
WRFZ	Wall Reverse Flow Zone
X/D	Dimensionless axial distance
λ	Excess air factor
α	The vane angle of the swirler, degree

1. Introduction

In the industrial applications, the combustion chambers consist mainly of three combustion zones after the inlet diffuser; the primary zone, where the major part of fuel combustion takes place and the flame being anchored in this zone, the intermediate zone, at which the dissociated products complete the combustion, and the dilution zone, at which the combustion products are diluted to meet the required turbine inlet temperature [1-3].

The primary zone airflow pattern has a significant function in the flame stabilization [4-7]. The common feature of the flow patterns used in combustors is the creation of swirling flows [8-11]. The swirling flow is clearly defined as a flow undergoing a concurrent or simultaneous axial, tangential, and vortex motions. The main important and desirable characteristic of swirl combustors is the formation of Central Reverse Flow Zone (CRFZ) and the central recirculation zones inside the combustor.

The recirculation zone has a main role in the flame stability process; the stabilization is accomplished by transferring some of the combustion products to be recirculated and to continually ignite the fuel air mixture [12-14].

In addition, CO, unburned fuel, and other intermediate species can reside within the combustor length and react to completion. The resulting mixture structure and the flame stabilization mechanism, obtained in the recirculation zone and induced by the air swirling motion, have significant effects on the combustion process control and the exhaust pollutants formation [15-18].

There are different ways for generating flow recirculation in the primary zone such as using air swirlers [19-20], bluff bodies [21-22], and opposed jet [23-24]. Air swirler creates very strong vortices through the air swirler blades located around the nozzle of the fuel inlet to establish a stabilized flame [25-27]. The hot gases are recirculated upstream toward the inlet fuel nozzle as a result of the creation of low-pressure zone at the combustor tube centerline and this results in the formation of swirling and tangential recirculation zones that stabilize and hold the flame. Swirling motion provides good mixing between the oxidizer or air and the inlet fuel which positively affects flame stability and enhances heat release rate and has a recognized effect on flame size and shape [28].

Many researchers have studied the diffusion flames and swirler designs; these studies include experimental and computational techniques to obtain results by analyzing the temperature distributions and velocity components at different operating conditions, in addition to measuring the concentration of pollutants in exhaust flow [29-33]. The renewable energy sources play an important role all over the world in reducing pollutants and using as alternative fuels as a result of fossil fuels depletion problem [34-40]. The previous review shows that, most researchers didn't employ the recent powerful techniques of flow visualization and complex computations available at the current modern CFD packages to understand the complicated flow dynamics and its relationship with combustion process.

So that, the present work studied in more details using numerical analysis, the effects of swirl number on gaseous fuel combustion characteristics and the cold flow field. It is clearly observed that the study of the flow field generated by the air swirler as a flame stabilizer is very important. The present study introduces cold and hot numerical studies on the air swirl number effects on the combustion characteristics of gaseous fuel. Also, the diffusion natural gas flame characteristics will be investigated using different swirl numbers and excess air factors.

2. Mathematical Model

In the present study, a Computational Fluid Dynamics (CFD) investigation for a 3D-turbulent swirl type combustor is introduced using ANSYS 14.5. The ANSYS package generally consists of different software programs, three of these programs have been used in the present study analysis, the first is the ANSYS Design Modeler which is used to construct the geometry, the second is ANSYS meshing which is used for mesh creation, and the third is ANSYS FLUENT which is used for solving the fluid mechanic, chemical reaction, heat transfer, and combustion calculations.

2.1. Model domain

The used combustion chamber model is a cylindrical tube 0.2 m inner diameter and one-meter length with a restricted end of the conical shape of 0.1 m length and 0.05 m exit diameter which is located at its end as illustrated in Fig. 1. The natural gas fuel nozzle of 0.01 m diameter is positioned at the swirler centre of the combustor tube as illustrated in Fig. 1. Air is introduced to the combustor through a swirler which has 16 uniform swirler blades with inner and outer diameters of 0.072 m and 0.1 m, respectively. In the present work, seven different air swirlers which have blade angles of 0° (S=0), 15° (S=0.23), 30° (S=0.5), 45° (S=0.87), 60° (S=1.5), 66° (S=2) and 74° (S=3) are used.

The swirl number is commonly used to indicate the swirl strength of the combustion air. The swirl number (S) of an annular swirler with constant setting vane angle ø can be determined from an expression given by Beer and Chigier [41] as shown:

S = (Angular Momentum . R_i) / (Linear momentum . R_o)

$$S = \frac{2}{3}\frac{\left[1-\left(\frac{R_i}{R_o}\right)^3\right]}{\left[1-\left(\frac{R_i}{R_o}\right)^2\right]}tan\,\alpha$$

Where R_i and R_o are the hub (inner) and outer radii of the swirler.

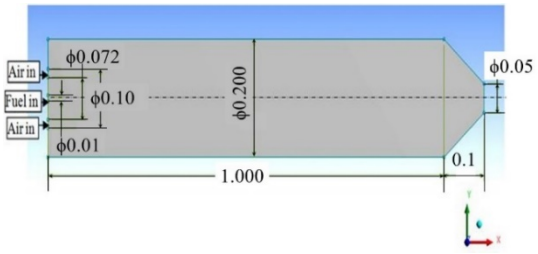

Fig. 1. The combustor model detailed dimensions in meters.

2.2. Mesh generation

ANSYS meshing application is used for generating the mesh cells inside the combustor model. The unstructured automatic mesh is created as shown in Fig. 2, using the tetrahedrons with patch conforming algorithm method. Mesh size is an important factor in mesh creation. When increasing the number of mesh cells, a more accurate solution will be obtained but more computing resources of memory and processing time will be required. In the present study, a fine mesh option is chosen to provide accurate results. In addition, successive rounds of mesh adaption in FLUENT solver are executed until

the solution became independent on the size and consequently independent of the mesh as shown in Fig. 3.

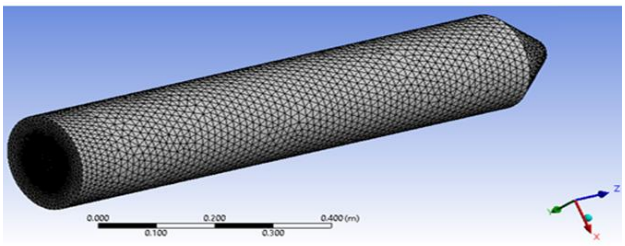

Fig. 2. Computational mesh of the combustor model.

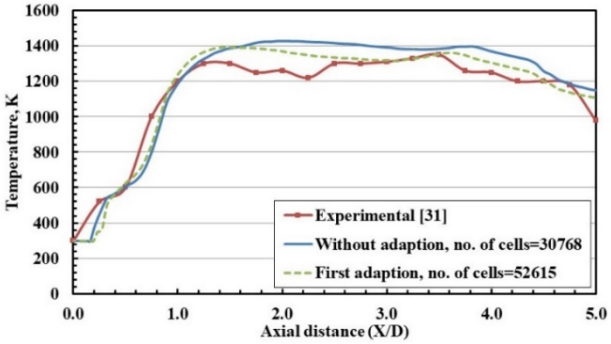

Fig. 3. The centerline axial flame temperature distributions for different meshes and no. of cells at S = 0.5 with A/F=30 (λ = 1.7).

2.3. Solver setting and turbulence model

Defining the solver setting and physics is considered as the final stage in the process of the CFD modelling. The physical setting of the used models such as the material general properties, model and domain characteristics are defined in ANSYS FLUENT.

In the present study, the steady state pressure-based solver is used. Because the main flow is not hypersonic, the energy equation model can be used, and a heat transfer can be modelled. P-1 radiation model is considered a practicable model because it can produce a fast and acceptable solution [42]. The results of many turbulence models are compared with the experimental results to obtain the suitable model. Fig. 4 shows that the SST k-ω model gives acceptable results which indicate a good agreement with the experimental results and closest to the results of the RSM model. The SST k-ω model takes less time for solution compared with RSM model. Also, the SST k-ω model was effectively developed with active blend and very accurate solution of the k-ω model in the regions close to the wall [43]. For the previous reasons, the SST k-ω is considered a suitable and applicable model that can be used for the numerical analysis in the present study.

In the present study, the non-premixed combustion model is used for combustion modelling as previously studied [44-47]. The study is carried out at the atmospheric pressure and exit pressure is defined as zero gauge. The boundary conditions are defined for the different physical model regions such as the inlet and outlet regions. Accurate and correct boundary conditions are very important for obtaining high accuracy in the CFD solution. The summary of the boundary conditions in the present study is clarified in the following table.

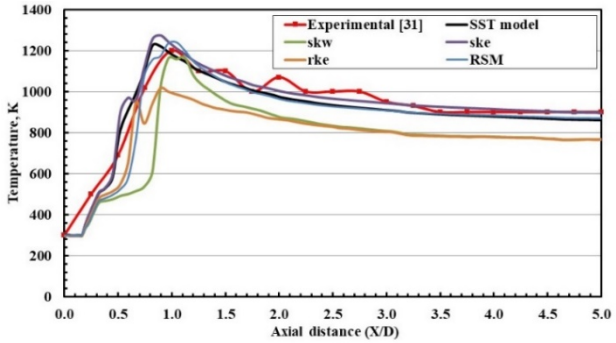

Fig. 4. The centerline axial flame temperature distributions for different turbulence models at S=0.87 and with A/F=50 (λ=2.9).

2.4. Model results

A 2D combustor model was created for the first simulation trial in the present study, but high error between the calculated and experimental results was found. So, the simulation analysis carried out in a complete 3D model to get a good agreement with the experimental measurements. In contrast with the 2D model, the 3D model requires longer computational time as a result of the large mesh numbers. The used combustor tube model has the advantage of being symmetrical around its axis. Also, the used flame stabilizer (air swirler) has 16 cyclic blades. From the previous analysis of the combustor model, only one-sixteenth section of the used combustor is modelled using the available periodic boundary conditions to simplify the model and decrease the computational time. The results obtained from this section are more accurate than those from the full 3D model because the mesh cell numbers increased which give better accuracy as illustrated in the following figures (Figs. 5 and 6).

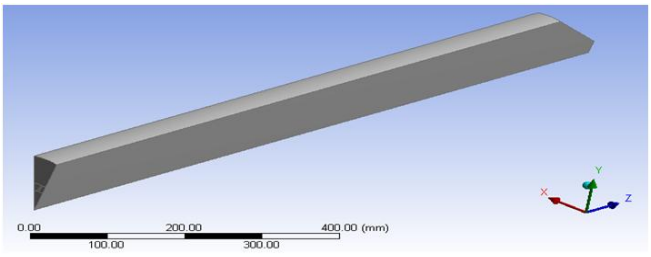

Fig. 5. One-sixteenth section flow model of the 3D combustor tube.

Table 1. The used boundary conditions

	Zone type	Flow Specification	Turbulence specification	T_{inlet}, K	Species
Fuel	Inlet mass flow	$\dot{m}_f$=0.4 g/s Axial velocity component = 1 Tangential velocity component = 0	Turbulence intensity = 7% Hydraulic diameter = 0.01 m	300	Mean mixture Fraction = 1
Primary air	Inlet mass flow	$\dot{m}_a$= Changed as run Axial velocity component = Changed as run Tangential velocity component = Changed as run	Turbulence intensity = 7% Hydraulic diameter = 0.028 m	300	Mean mixture Fraction = 0
Outlet	Pressure outlet	Backflow directions specification: Normal to boundary Radial equilibrium pressure distribution	Turbulence intensity = 7% Hydraulic diameter = 0.05 m	300	Mean mixture fraction = 0

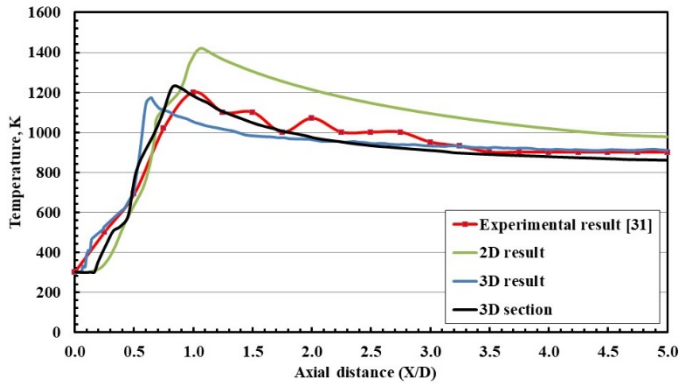

Fig. 6. The centerline axial temperature distributions of the experimental data, 2D, full 3D, and 3D-section numerical data at S=0.87 and with A/F=50 (λ=2.9).

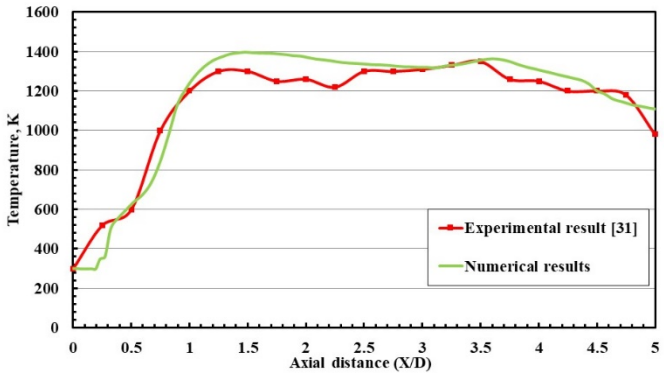

Fig. 7. A comparison between experimental and numerical results of the flame centerline axial temperatures at S=0.5 and with A/F=30 (λ=1.7).

2.5. Validation of computation

In order to validate the computational procedure, comparison of the present calculations with the experimental data [31] was performed. The combustor model tube used in the present study for the model validation has the same geometrical dimensions of that used for experimental results under the same operating conditions. In the numerical simulation model combustor as previously discussed, a periodic boundary conditions can be enabled to only one-sixteenth section of the combustor model. Figures 7 and 8 show detailed comparisons between the experimental results and the current numerical results in terms of the axial flame temperatures at the combustor centerline. It is clearly observed that there is a good agreement between the numerical and experimental results.

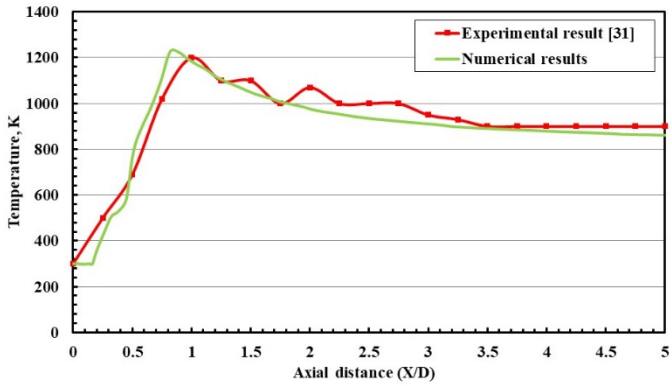

Fig. 8. A comparison between experimental and numerical results of the flame centerline axial temperatures at S=0.87 and with A/F=50 (λ=2.9).

3. Results and Discussion

3.1. Effect of swirl number on flow pattern

The effects of the air swirl numbers on the flow pattern inside the swirl combustor are investigated. The air swirl number is changed as S = 0, 0.23, 0.5, 0.87, 1.5, 2 and 3 by using seven air swirlers having the same dimensions but differ in the swirler vane angles which are 0°, 15°, 30°, 45°, 60°, 66° and 74° respectively. The calculations are carried out firstly at cold flow with two different air mass flow rates ($\dot{m}_a$) equal 13.7 and 27.5 g/s then carried out later with excess air factor (λ) = 2 and 4 keeping the natural gas fuel mass flow rate constant at 0.40 g/s. The effect of air swirl number on the flow pattern with and without combustion is studied for describing the Reverse Flow Zone (RFZ) boundary, recirculated flow mass ratio, flow pathlines, and vortex eye location.

The velocity distribution inside the combustor is very important in studying the combustion flow pattern, especially the axial flow velocity inside the reverse flow zone. This is important in keeping the flow of the combustion gases at a low velocity that acts as a heat source or spark initiation for the introduced fresh mixture of fuel and air. To present the numerical results in the present work, the axial velocity distribution maps are obtained by representing the velocity at different ranges by coloured regions on a flat plane passing through the combustor centerline.

(i) Effect of swirl number on RFZ boundary

The air swirler has a main function as it enhances the diffusion flame stability as it forms the recirculation zones at which the circulated mass gives fast mixing between the fuel and the oxidant. The trace of points that have zero axial velocity divides the flow field into two zones which are the forward flow zone and reverse flow zone (RFZ) with respect to the main flow direction. The trace of these points is named as the boundary of RFZ. This can be achieved by determining the positions at which the axial velocity equals zero under the different operating conditions.

The air swirl number effects on RFZ boundary with and without combustion are shown in Figs. 9 to 11. At cold flow, for S = 0, a small size of RFZ is formed at the combustor centerline attached to the air swirler because of the swirler hub diameter (0.072 m) acting as a bluff disc. By increasing swirl number to 0.23, additional small RFZ is formed at axial distance X/D = 0.9 from the swirler. By further increase of the swirl number, the RFZ takes the shape of an ellipsoid where its size increases in diameter through the axial length of the combustor far from the air swirler to reach its maximum diameter, then decreases at a certain position of the combustor axial distance. This reverse flow zone is called the Central Reverse Flow Zone (CRFZ) which is created due to the swirling motion added to the inlet flow by the axial swirler. The size of the CRFZ grows in both axial and radial directions and its length increases and shifts closer to combustor tube end and the location of the stagnation point moves downstream when increasing the air swirl number, but the CRFZ fails to reach the combustor model tube exit as a result of the end restriction. Also, the bottom of the CRFZ increased in diameter and becomes more attached to the combustor upstream with increasing the swirl number. Another RFZ attached to the combustor corner is formed and called the Wall Reverse Flow Zone (WRFZ). The WRFZ is formed due to the abrupt expansion of the flow into the combustor and its size decreases until disappearing when the air swirl number increased.

The effect of changing swirl number at cold flow is the same as in combusting flow. However, due to the fuel jet, a forward narrow flow zone around the combustor tube axis and downstream of the fuel inlet nozzle penetrates the CRFZ. This region or zone shifts close to the centerline due to the higher momentum values of the reserved flow masses when compared with that of the fuel jet. Also, it is found that the size of the CRFZ decreases in the case of combustion, because the thermal expansion that took place in the forward flow region results in increasing the volumetric flow rate. The thermal expansion occurred also inside the CRFZ, but with smaller effect in contrast with that occurred in the forward flow region, as shown in Fig. 11.

(ii) Effect of swirl number on recirculated flow mass ratio

Most combustion systems such as gas turbine combustors involve large regions of recirculating flows. These zones provide a heat source, by upstream convection and hot circulated combustion products gases mixing with fresh inlet air and fuel streams, to serve as a source of continues ignition. The circulation zone size strongly affects the production rate of hot products and consequently the heat release rate from the combustion process. In addition, this affects the thermal efficiency.

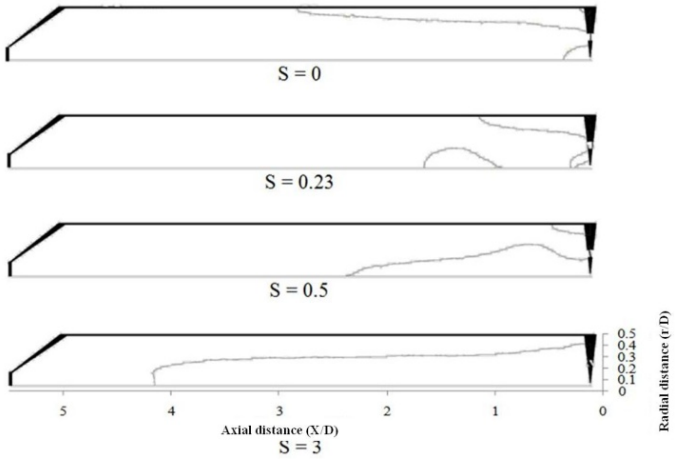

Fig. 9. The effect of the air swirl number on the RFZ boundaries at $\dot{m}_a$= 13.7 g/s [Without combustion].

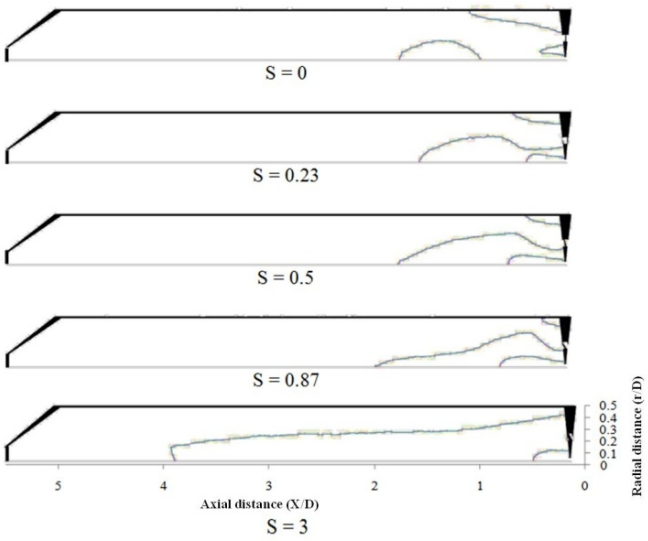

Fig. 10. The effect of the air swirl number on the RFZ boundaries at λ = 4 [With combustion].

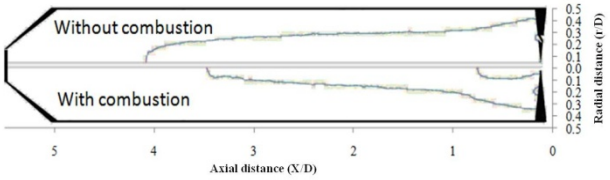

Fig. 11. Comparison between the RFZ boundaries at S = 2 [without combustion at $\dot{m}_a$= 13.7 g/s and with combustion at λ = 2 ($\dot{m}_a$= 13.7 g/s and $\dot{m}_f$= 0.4 g/s)].

The recirculated flow mass ratio inside the circulation zone to the inlet flow mass is numerically calculated for three different sectional surfaces at which axial distances of X/D = 1, 2.5 and 3.5 through the length of the combustor tube model. The reversed mass flow rates [$\dot{m}_r$] that are passing through these planes are calculated and divided to the total inlet flow [$\dot{m}_i$] and plotted as shown in Fig. 12 at cold and combusting flows. The recirculated mass ratio increased when the swirl number increased at the three planes but at small swirl numbers, the mass ratio has a small or zero value due to the absence of the RFZ. At axial distance X/D = 1 and λ = 4, the value of the recirculated flow mass ratio at S = 0.87 is lower than that at S = 0.23 and at S = 0.5, this exceptional behavior is due to that the CRFZ tends to get longer and thinner starting from S = 0.87 which leads to less reversed mass flow at X/D = 1.

(iii) Effect of swirl number on the flow pathlines

The flow pathlines are used in the present study for visualizing the swirl flow motion which includes the circulation zone, the RFZ, and the position or location of the vortex eye. The pathlines are the lines which travels by buoyant particles in the equilibrium with the fluid stream motion. Pathlines are produced from ANSYS FLUENT program. Based on the relative velocities, the pathlines are identical to the streamlines.

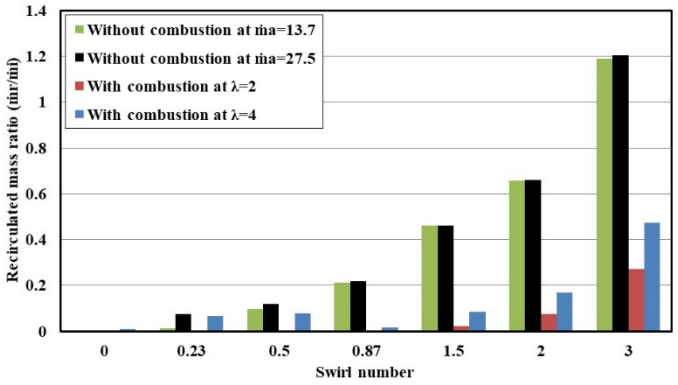

[a] X/D=1

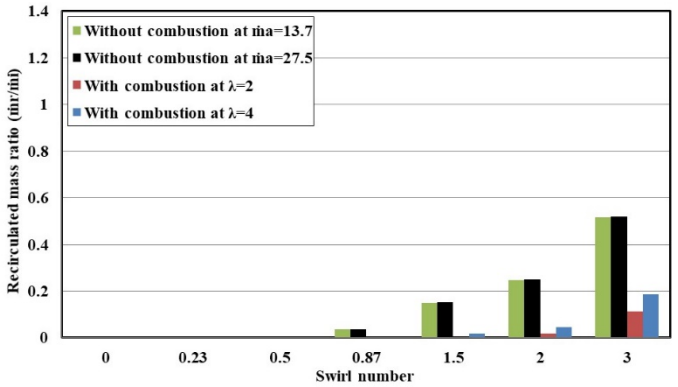

[b] X/D=2.5

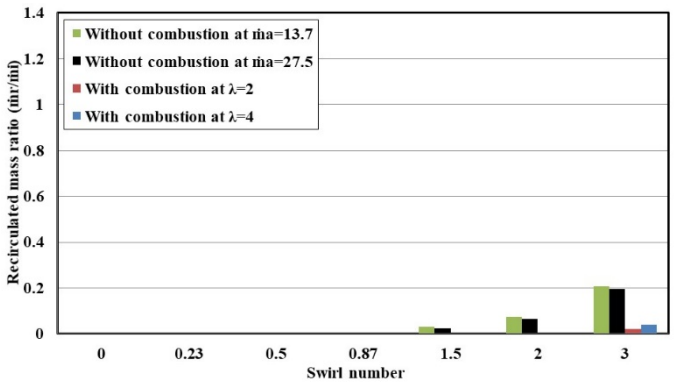

[c] X/D=3.5

Fig. 12. The effect of the air swirl number on recirculated mass flow ratio without combustion at $\dot{m}_a$= 13.7 and 27.5 g/s and with combustion at λ = 2 and 4.

Figures 13 and 14 show the pathlines of the flow with and without combustion. At low swirl number (<0.5), the effect of the corner vortex is dominated while a small central vortex is formed due to the CRFZ effect. By increasing the swirl number, the size of the corner vortex decreases until disappearing while the central vortex size is increased and gets larger. At combusting flow, an additional vortex eye is observed due to the axial fuel flow jet that penetrates the CRFZ; this vortex eye location is almost the same under the different swirl numbers.

By comparing the flow pathlines with and without combustion at the same swirl number, it is found that the size of the central vortex decreased in case of combustion, because the thermal expansion occurs in the forward flow region and inside the reverse flow zone. The effect of thermal expansion inside the reverse flow zone is smaller than that in forward flow region, this thermal expansion increases the volumetric flow rate.

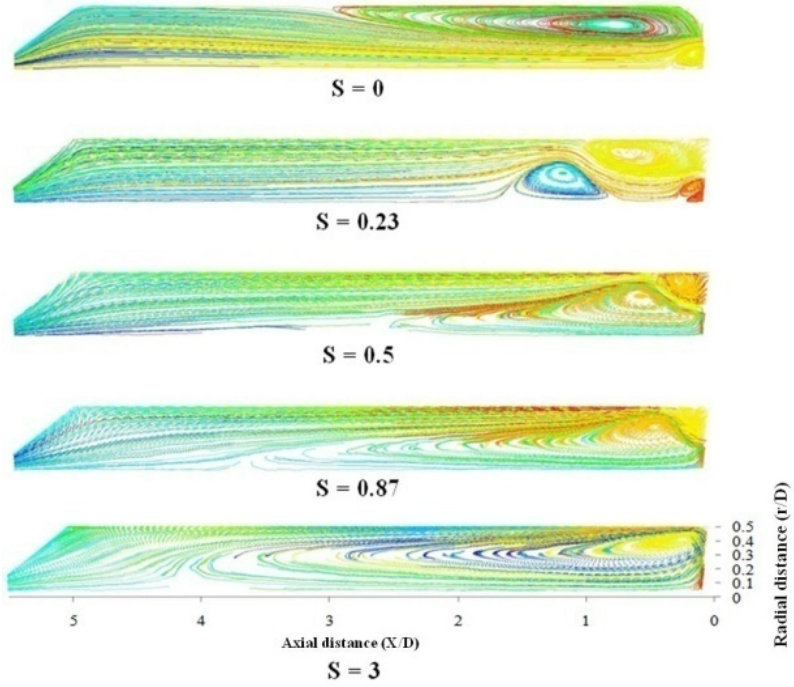

Fig. 13. The effect of the air swirl number on the flow pathlines at $\dot{m}_a$= 13.7 g/s [without combustion].

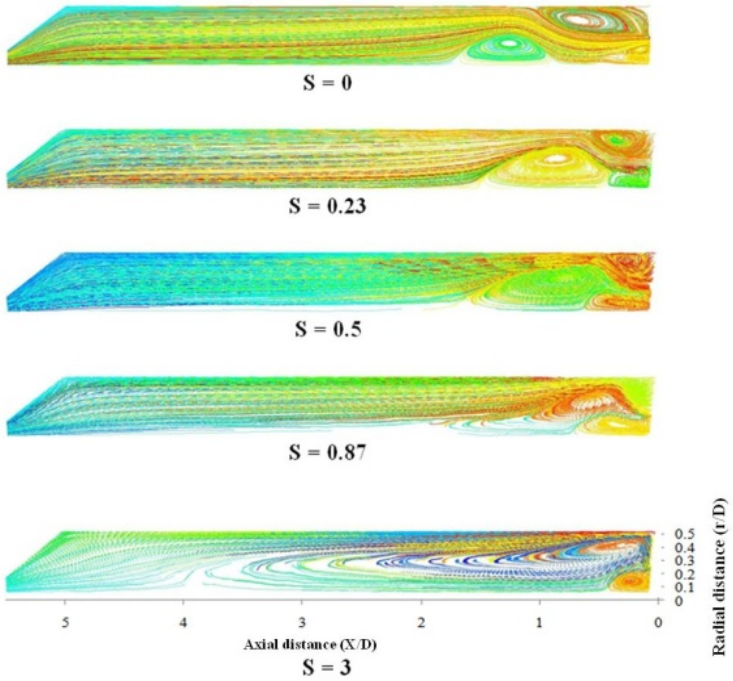

Fig. 14. The effect of the air swirl number on the flow pathlines at λ = 4 [with combustion].

(iv) Effect of swirl number on vortex eye location

The vortex eye is defined as the center of the recirculation zone around which the streamline moves. The location of the central vortex eye is shifted outward to the combustor wall by increasing swirl number as shown in Figs. 15 and 16. This movement is due to the stronger swirling action and tangential momentum that forces the inlet flow in the radial direction to the combustor corner. Increasing the swirl number increases the tangential velocity while decreases the axial velocity which leads moving the vortex eye upstream (to the burner head) and outward (to the combustor wall). This shift is considered as an indication for the shape of the RFZ and its boundaries. Shifting the vortex eye close to the burner head (upstream) indicates that the flame will be also close to the burner head with small length and size which means that a small combustion chamber can be used.

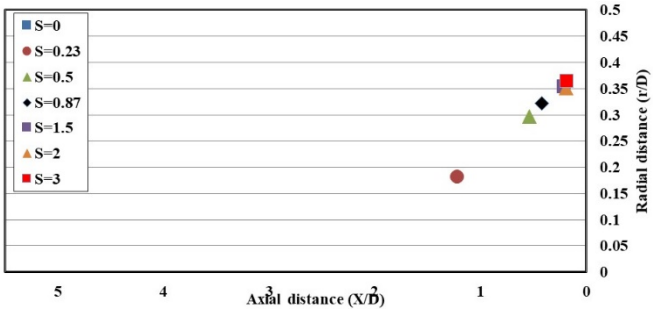

Fig. 15. The effect of the air swirl number on the central vortex eye location at $\dot{m}_a$= 13.7 g/s [without combustion].

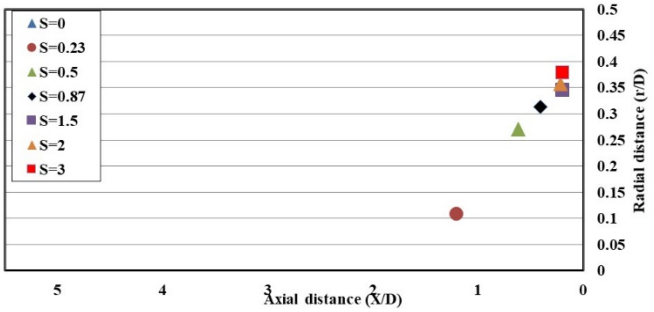

Fig. 16. The effect of the air swirl number on the central vortex eye location at λ = 2 [with combustion].

3.2. Effects of air swirl number on temperatures distribution and species concentrations

In the following sub-sections, the effects of the air swirl numbers on the natural gas flame characteristics such as the flame temperatures distributions and species concentrations are illustrated for different excess air factors.

(i) Effect of air swirl number on temperatures distributions

The flames temperature maps are plotted for natural gas combustion for excess air factors of 2 and 4 when the fuel mass flow rate is kept constant at 0.4 g/s. From Fig. 17, for weak swirl [S ≤ 0.5], the temperature levels are relatively high, and the high-temperature regions have larger sizes than those at strong swirl for the same excess air factor. When the swirl number is increased, the flame high temperatures region is shifted upstream close to the burner head. It can be observed that, when the swirl number increased, the circulation zone became stronger, i.e., the recirculated air mass flow rate increased and the mixing rate also increased and consequently it gives flames with small sizes, i.e., shorter in length and wider in diameter. This result indicates that, in this case, a compact combustion chamber can be used.

The flames temperatures levels are lower with the higher air swirl numbers because the flame high temperatures regions shift upstream, and this leads to a flame with a shorter length. Also, the average gases temperature at the combustor tube end is decreased by increasing the swirl number. The outlet gases temperature decreased by about 30 % and 20 % when the swirl number increased from 0 to 3 at λ = 2 and 4, respectively as shown in Fig. 18.

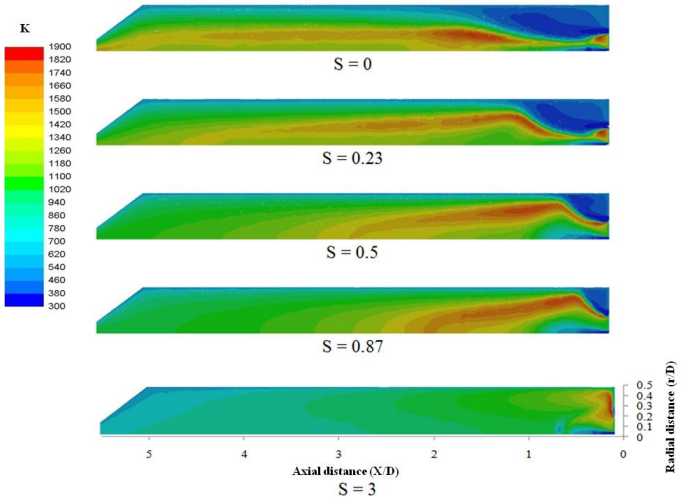

Fig. 17. The effect of the swirl number on the flame temperatures maps at λ = 2.

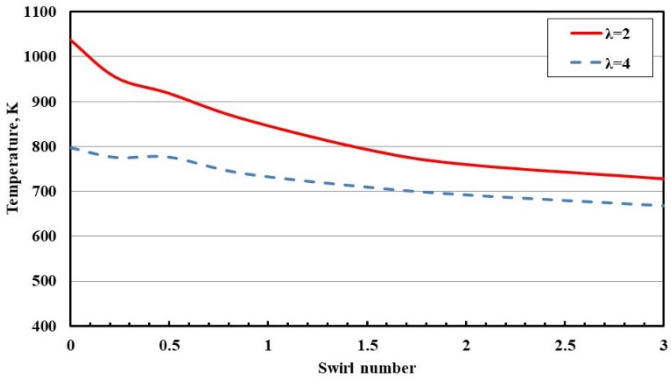

Fig. 18. The effect of the air swirl number on the average gases temperature at the combustor tube outlet.

(ii) Effects of swirl number on the species concentrations

The effect of the air swirl number on the species concentration, including CO, O_2, CO_2, CH_4, is studied using the mole fraction maps and combustor average outlet values for λ equals 2 and 4 while the fuel mass flow rate is kept constant at 0.40 g/s as shown in Figs. 19 to 22. The concentration of CO is high at the weak swirl and is decreased gradually by increasing the swirl number and shifted upstream. The average CO concentrations at the combustor tube outlet decreased by about 100 % when the air swirl number increased from 0 to 1.5 at λ = 2 and by about 100 % also when the swirl number increased from 0 to 0.87 at λ = 4. The decrease in the CO concentrations when the swirl number increased is because the combustion process is improved, and this tends to reach the complete combustion.

The concentration of O_2 is low at the combustor centerline and combustor upstream near the swirler because most of the present O_2 is consumed in the combustion. The O_2 concentrations increased gradually axially through the combustor length starting from a certain location downstream of the combustor as an indication of the end of the chemical reaction. This location moves upstream with the movement of the flame by increasing the swirl number. In addition, increasing the swirl number also increases the O_2 concentration mole fraction while the values of CO_2 concentrations are decreased and move upstream with increasing the swirl number. The CO_2 concentrations at the combustor outlet are nearly constant for higher swirl numbers.

The concentration of CH_4 is decreased with the axial distance from the burner head. The length of CH_4 penetration decreases and shifts upstream the combustor with increasing the swirl number and excess air factor. This is due to improving the combustion of the fuel as the swirl number increases. The average unburned fuel (CH_4) concentration, exiting from the combustor tube, decreased by about 100 % when the swirl number increased from 0.0 to 1.5 with λ = 2 and by 100 % also when the air swirl number increased from 0.0 to 0.87 with λ = 4.

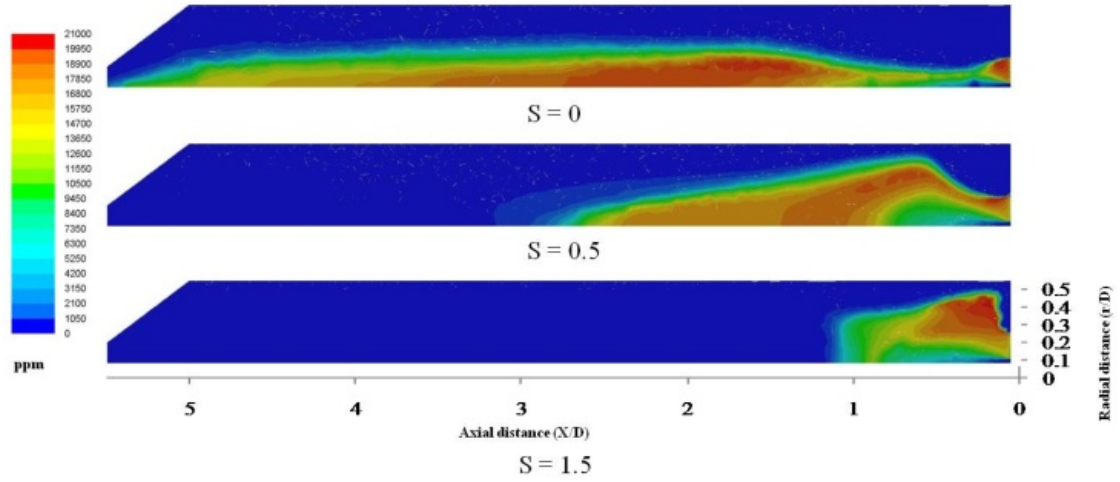

Fig. 19. The effect of the swirl number on the CO concentrations with λ = 2.

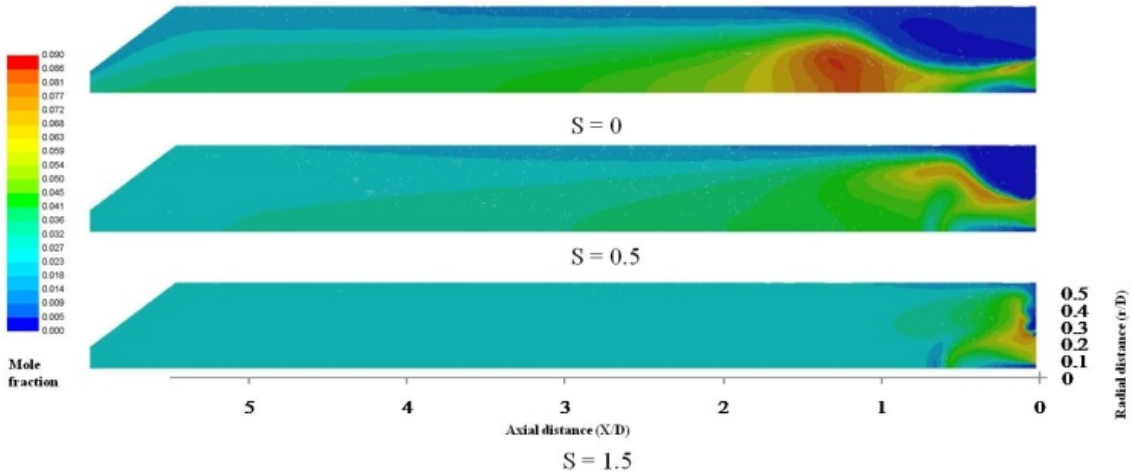

Fig. 20. The effect of the swirl number on the CO_2 concentrations with λ = 2.

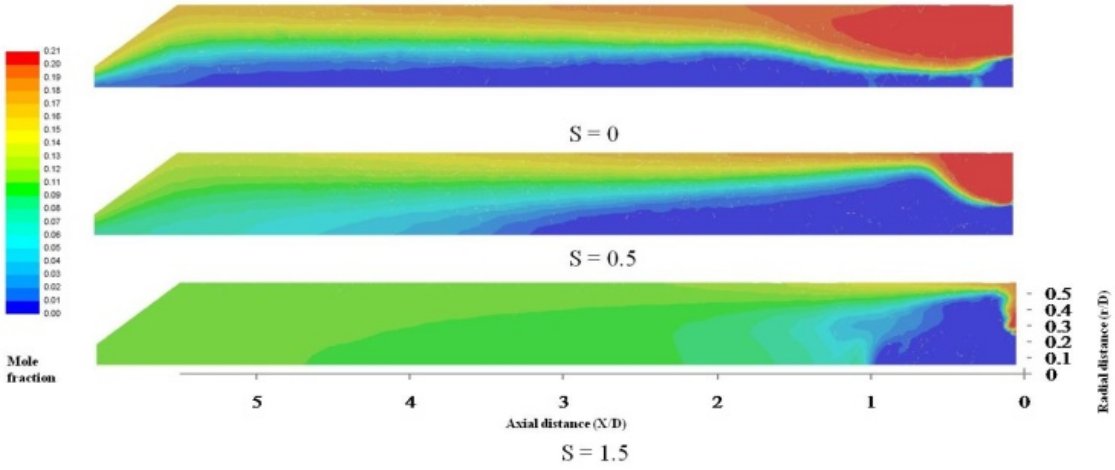

Fig. 21. The effect of the air swirl number on the O_2 concentrations with $\lambda = 2$.

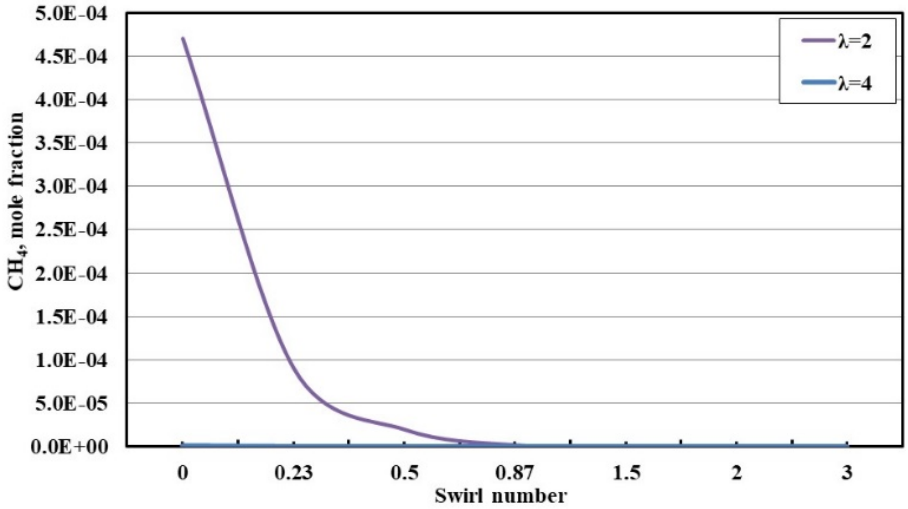

Fig. 22. The effect of the air swirl number on the average unburned fuel (CH_4) concentrations at the combustor tube end.

4. Conclusion

The present study focuses on the numerical investigation of the swirling flow field characteristics with/without combustion. The effects of the air swirl number and the excess air factor are studied on the RFZ, the circulated flow mass ratio, the flow pathlines, vortex eye positions or locations, the diffusion flame temperatures distribution, and concentrations percentages of the combustion products. The air swirl number is varied from 0 to 3 considering the gaseous fuel as natural gas with a constant mass flow rate of 0.40 g/s. Also, the excess air factor is changed as 2 and 4 in the combustion case. The obtained conclusions can be summarized in the following:

1 - Comparing the experimental and calculated axial temperatures distributions at the same operating conditions, a good agreement is found.

2 - Comparing the experimental and calculated axial centerline temperatures distribution using full 3D, and 3D section a reasonable agreement is found.

3 - Increase the air swirl number leads to:

- Increasing the size of the CRFZ in both length and diameter while decreasing in the size of the wall reverse flow zone until disappearing.
- Increasing the circulated mass ratio.
- Decreasing the size of the corner vortex until disappearing while increasing the size of the central vortex and shifting the location of the central vortex eye to the combustor corner.
- Decreasing the flame length and lowering the temperature levels.
- Decreasing the concentration of CO and unburnt CH_4.

4- The average temperature at the combustor tube end is decreased by about 30 % and 20 % by increasing the air swirl number from 0 to 3 at $\lambda = 2$ and 4, respectively.

References

[1] I. Glassman and R. A. Yetter, Combustion (Fourth Edition), Elsevier, 2008.

[2] A. H. Lefebvre and D. R. Ballal, Gas Turbine Combustion Alternative Fuels and Emissions, Taylor and Francis Group, LLC, 2010.

[3] F. El-mahallawy and S. E. Habik, Fundamentals and Technology of Combustion, Elsevier, 2002.

[4] J. Matthes, P. Waibel, M. Vogelbacher, H.-J. Gehrmann, H.B. Keller, "A new camera-based method for measuring the flame stability of nonoscillating and oscillating combustions", Experimental Thermal and Fluid Science 105, pp. 27-34, 2019.

[5] A. Kaewpradap and S. Jugjai, "Experimental study of flame stability enhancement on lean premixed combustion of a synthetic natural gas in Thailand", Energy 188, pp. 1-10, 2019.

[6] S. A. Said, M. Aliyu, M. A. Nemitallah, M. A. Habib, I. B. Mansir, "Experimental investigation of the stability of a turbulent diffusion flame in a gas turbine combustor", Energy 157, pp. 904-913, 2018.

[7] M. A. Nemitallah, B. Imteyaz, A. Abdelhafez, M. A. Habib, "Experimental and computational study on stability characteristics of hydrogen-enriched oxy-methane premixed flames", Applied Energy 250, pp. 433–443, 2019.

[8] A. Giannadakis, A. Naxakis, A. Romeos, K. Perrakis and Th. Panidis, "An experimental study on a coaxial flow with inner swirl: Vortex evolution and flow field mixing attributes", Aerospace Science and Technology 94, p. 1-16, 2019.

[9] P. Singh, R. K. Velamati, C. Prathap, A. Mohammad, S. Chander, "Study of flow patterns and impingement heat transfer for an annular array of eight co-rotating dual-swirling flames", International Journal of Heat and Mass Transfer 144, pp. 1-16, 2019.

[10] N. Kharoua, L. Khezzar, M. Alshehhi, "The interaction of confined swirling flow with a conical bluff body: Numerical simulation", Chemical Engineering Research and Design 136, pp. 207-218, 2018.

[11] L. Liu, B. Bai, "A mechanistic model for the prediction of swirling annular flow pattern transition", Chemical Engineering Science 199, pp. 405-416, 2019.

[12] L. Yan, W. Song, D. Xu, J. Chen, "Effect of heat recirculation on the combustion stability of methane-air mixtures in catalytic micro-combustors", Applied Thermal Engineering 115, pp. 702–714, 2017.

[13] F. Song, Z. Wen, Z. Dong, E. Wang, X. Liu, "Numerical study and optimization of a porous burner with annular heat recirculation", Applied Thermal Engineering 157, pp. 1-11, 2019.

[14] Y. Tu, A. Zhou, M. Xu, W. Yang, K. B. Siah, S. Prabakaran, "Experimental and numerical study on the combustion of a 32 MW wood-chip grate boiler with internal flue gas recirculation technology", Energy Procedia 143, pp. 591-598, 2017.

[15] H. Zhou, S. Meng, "Numerical prediction of swirl burner geometry effects on NOx emission and combustion instability in heavy oil-fired boiler", Applied Thermal Engineering 159, pp. 1-10, 2019.

[16] K. Hab, V. Medina, A. Okon, C. CT, "Combustion and emission performance of CO2/CH4/biodiesel and CO2/CH4/diesel blends in a Swirl Burner Generator", Energy Procedia 142, pp. 154–159, 2017.

[17] A. M. Elbaz, H. A. Moneib, K. M. Shebil, W. L. Roberts, "Low NOX - LPG staged combustion double swirl flames", Renewable Energy 138, pp. 303-315, 2019.

[18] N. Motamedifar, A. Shirneshan, "An experimental study of emission characteristics from cylindrical furnace: Effects of using diesel-ethanol-biodiesel blends and air swirl" Fuel 221, pp. 233–239, 2018.

[19] L. Palanti, D. Pampaloni, A. Andreini, B. Facchini, "Numerical simulation of a swirl stabilized methane-air flame with an automatic meshing CFD solver", Energy Procedia 148, pp. 376–383, 2018.

[20] M. M. Torkzadeh, F. Bolourchifard, E. Amani, "An investigation of air-swirl design criteria for gas turbine combustors through a multi-objective CFD optimization", Fuel 186, pp. 734–749, 2016.

[21] Y. J. Kim, B. J. Lee, H. G. Im, "Hydrodynamic and chemical scaling for blow-off dynamics of lean premixed flames stabilized on a meso-scale bluff-body" Proceedings of the Combustion Institute 37, pp. 1831–1841, 2019.

[22] Y. Tong, X. Liu, S. Chen, Z. Li, J. Klingmann, "Effects of the position of a bluff-body on the diffusion flames: A combined experimental and numerical study", Applied Thermal Engineering 131, pp. 507–521, 2018.

[23] H. Y. Shih, J. R. Hsu, "A computational study of combustion and extinction of opposed-jet syngas diffusion flames", international journal of hydrogen energy 36, pp. 15868-15879, 2011.

[24] J. Carpio, A. le Liñán, A. L. Sánchez, F. A. Williams, "Aerodynamics of Axisymmetric counter flowing jets", Combustion and Flame 177, pp. 137–143, 2017.

[25] S. Chen and D. Zhao, "Numerical Study of Non-reacting Flow Fields of a Swirling Trapped Vortex Ramjet

Combustor", Aerospace Science and Technology 74, pp. 81–92, 2018.

[26] X. Liu, A. M. Elbaz, C. Gong, X. S. Bai, H. T. Zheng, W. L. Roberts, "Effect of Burner Geometry on Swirl Stabilized Methane/Air Flames: A Joint LES/OH-PLIF/PIV Study", Fuel 207, pp. 533–546, 2017.

[27] L. Y. Wang, S. Chatterjee, Q. An, A. M. Steinberg, Ö. L. Gülder, "Soot Formation and Flame Structure in Swirl-Stabilized Turbulent Non-Premixed Methane Combustion", Combustion and Flame 209, pp. 303–312, 2019.

[28] P. Kiameh, "Power Generation Handbook", McGraw-Hill Professional, 2002.

[29] V. Patel and R. Shah, "Effect of swirl and number of swirler vanes on combustion characteristics of methane inverse diffusion flame", Journal of Mechanical Science and Technology, Vol. 33, 2019.

[30] M. İlbaş, S. Karyeyen and İ. Yilmaz, "Effect of swirl number on combustion characteristics of hydrogen-containing fuels in a combustor", International Journal of Hydrogen Energy, Vol. 41, 2016.

[31] A. I. A. Farag, "Study of secondary air effect on natural gas combustion characteristics", Ph.D. thesis, Port Said University, Egypt, 2012.

[32] Y. Belal, G. Li, Z. Zhang, H. M. El-Batsh, H. A. Moneib and A. M. A. Attia, "The effect of swirl burner design configuration on combustion and emission characteristics of lean pre-vaporized premixed flames", Energy, Vol. 228, 2021.

[33] N.J. Bai, W.J. Fan, R.C. Zhang, Z.P. Zou, C.X. Zhang and P.L. Yan, "Numerical investigation into the structural characteristics of a hydrogen dual-swirl combustor with slight temperature rise combustion", International Journal of Hydrogen Energy, Vol. 46, 2021.

[34] K. D. L. C. Hoz, J. F. Pérez and E. L. C. Arrieta, "Design of a top-lit up-draft micro gasifier biomass cookstove by thermodynamic analysis and fluent modeling", International journal of renewable energy research (IJRER), Vol. 7, pp. 2172-2187, 2017.

[35] B. Khalida, Z. Mohamed, S. Belaid, H. O. Samir, K. Sobhi and S. Midane, "Prediction of Higher Heating Value HHV of Date Palm Biomass Fuel using Artificial Intelligence Method", 8th International Conference on Renewable Energy Research and Applications (ICRERA), pp. 59-62, November 2019.

[36] N. Campagna, M. Caruso, V. Castiglia, R. Miceli and F. Viola, "Energy Management Concepts for the Evolution of Smart Grids", 8th International Conference on Smart Grid (icSmartGrid), pp. 208-213, 2020.

[37] F. Ayadi, I. Colak, I. Garip, and H. Bulbul, "Impacts of Renewable Energy Resources in Smart Grid", 8th International Conference on Smart Grid (icSmartGrid), June 2020.

[38] A. M. Salman, I. A. Ibrahim, H. M. Gad, and T. M. Farag, "Effects of Air Temperature on Combustion Characteristics of LPG Diffusion Flame", Materials Science Forum, Vol. 1008, pp. 128-138, 2020.

[39] L. F. N. Lourenço, N. Suzuki, R. M. Monaro and M. B. C. Salles, "Economical Evaluation of an Isolated AC Offshore Grid for Pre-salt Oil Production Based on Power Hub for Reducing Carbon Emissions", 8th International Conference on Renewable Energy Research and Applications (ICRERA), pp. 450-454, 2019.

[40] D. Icaza and D. Borge-Diez, "Potential Sources of Renewable Energy for the Energy Supply in the City of Cuenca-Ecuador with Towards a Smart Grid", 8th International Conference on Renewable Energy Research and Applications (ICRERA), pp. 603-610, November 2019.

[41] J. M. Beer and Chigier, "Combustion aerodynamics", Applied Science Publishers, London, 1972.

[42] I. Yılmaz, M. Tastan, M. Ilbas and C. Tarhan, "Effect of Turbulence and Radiation Models on Combustion Characteristics in Propane–Hydrogen Diffusion Flames", Energy Conversion and Management, Vol. 72, pp. 179–186, 2013.

[43] ANSYS Fluent theory guide, 2009.

[44] M. Ilbas, "The effect of thermal radiation and radiation models on hydrogen –hydrocarbon combustion modelling", Int. J. of Hydrogen Energy, Vol. 30, pp. 1113-1126, 2005.

[45] M. Ilbas, I. Yilmaz and Y. Kaplan, "Investigation of hydrogen and hydrogen-hydrocarbon composite fuel combustion and NOx emissions characteristics in a model combustor", Int. J. of Hydrogen Energy, Vol. 30, pp. 1139-1147, 2005.

[46] I. A. Ibrahim and M. M. Shabaan, "Numerical Simulation of Methane Combustion with and without Radiation Models", PSERJ, Vol. 17, No. 1, March 2013.

[47] I. A. Ibrahim, T. M. Farag, M. A. Shehata and M. M. Shabaan, "Flow Field and Combustion Characteristics of Natural Gas inside a Gas Turbine Combustor", Port Said Engineering Research Journal, Vol. 17, No. 2, pp. 18-29, 2013.